Memoirs of the Faculty of Engineering, Kyushu University, Vol.65, No.4, December 2005

Development of a Laser-Guided Deep-Hole Internal-Grinding Tool (Series 1): Grinding Forces

by

Akio KATSUKI[*], Hiromichi ONIKURA[**], Takao SAJIMA[*]
and Hyunkoo PARK[***]

(Received November 7, 2005)

Abstract

The laser-guided deep-hole internal grinding tool is developed to bore accurate and straight deep-holes with high surface quality. The tool consists of a grinding head, the front and rear actuators mounted on an actuator holder and a laser diode set in the back end of the holder. The grinding head consists of a diamond or CBN wheel, an air motor, and the piezoelectric actuators for the compensation of tool diameter. The grinding wheel is located eccentrically at the grinding head. The grinding is performed by the rotation of the grinding wheel and the rotation of the grinding head. In this paper, with the grinding forces, it is examined whether the air motor, which is used in the developed grinding head, can be used sufficiently as grinding motor. Further it is examined that the displacement of a grinding motor can be compensated by piezoelectric actuators, which are set up in the grinding head. The relationship between grinding torques and hole deviations during internal grinding of hardened steel S45C are examined and it is cleared that the developed grinding head can be used for finishing the deep hole when a depth of cut is small.

Keywords: Deep hole, Internal grinding, Grinding force, Guide pad, Diamond wheel, Piezoelectric actuator, Compensation of grinding tool diameter

1. Introduction

Deep holes with a hole depth L to diameter D ratio of more than 5 are bored in hydraulic

[*] Research Associate, Department of Intelligent Machinery & Systems
[**] Professor, Department of Intelligent Machinery & Systems
[***] Graduate Student, Department of Intelligent Machinery & Systems

cylinders, landing gears for aircraft, oil industry components and injection molding machinery etc[1] .

Gun drills, BTA (Boring and Trepanning Association) tools and ejector drills are used to bore deep holes of high length-to-diameter ratio. The gun drills are used for a small size hole and the BTA tools or ejector drills are used for a large size hole. More accurate holes can be bored using these tools as compared to twist drills by the self-guidance of their guide pads.

However, it is difficult and limited that hole accuracies are improved without controlling of the tools. Recently, many approaches have been made to improve the accuracies of deep-hole. Katsuki et al. develops a high-performance laser-guided deep-hole boring tool[2),3)] . B.K. Min et al. develops a boring tool for improving the accuracy and flexibility of line boring in the automotive industry[4)]. The boring tool is controlled using a laser position sensor and a piezoelectric actuator. W.M. Chiu et al. researches the compensation of the tool displacement using a computer-controlled piezoelectric actuator on the boring bar holder[5)].

In the internal grinding, it is very difficult to finish deep-hole without control of the grinding head. Because the stiffness of the shaft of a grinding wheel decreases as the depth of hole increases. Therefore, the laser-guided deep-hole internal grinding tool is developed. To evaluate performance of the developed tool, the following model experiments are carried out. In the first model experiment on the NC milling machine, the grinding forces are examined to clarify whether the performance of an air motor is sufficient. In the second model experiment on the NC milling machine, the displacement of a grinding motor, the stiffness of an air motor spindle and performance of piezoelectric actuators to compensate the displacement of grinding motor are examined. In the third model experiment on the lathe, the internal grinding is carried out to examine the grinding condition in the deep hole.

2. Structure of System

To bore precise deep holes, the laser-guided deep-hole internal grinding system is designed. The system is shown in **Fig.1**. The system consists of an apparatus ⑱ for setting a guiding axis, the developed tool, a laser diode ⑦, a double disk coupling ③ for prevention of tool rolling and two PSDs (Position-Sensitive Detector) ⑯, ⑰.

The laser-guided deep-hole internal grinding tool is shown in **Fig.2**. The tool consists of a grinding head, an actuator holder setting piezoelectric actuators and the laser diode.

The grinding head has an inner case. The air motor with a grinding wheel is set up into the inner case. The inner case is set eccentrically to adjust the tool diameter to110mm, as shown in **section A**. Guide pads are located asymmetrically around the grinding head. The grinding forces

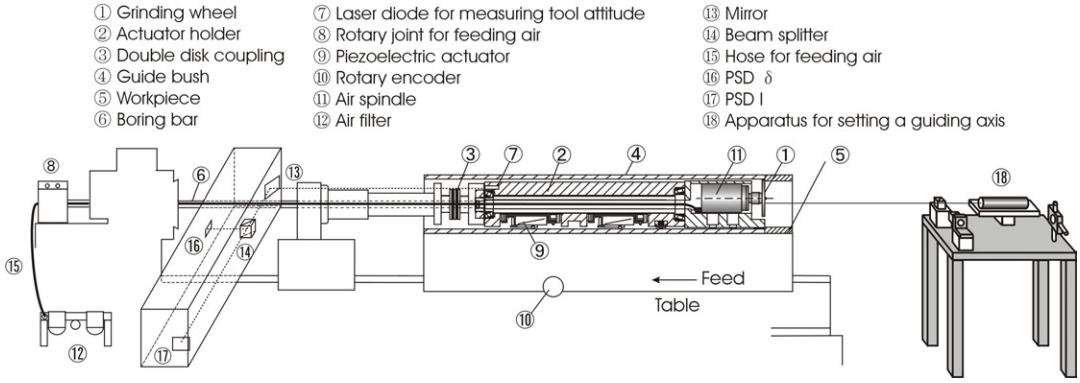

Fig. 1 Laser-guided deep-hole internal grinding system.

acting on the grinding wheel are counterbalanced by guide pads after the grinding head has entered the workpiece. By this operation of the guide pads, the internal grinding can be carried out stably. And two piezoelectric actuators are placed under the inner case. These actuators are used to adjust tool diameter to110mm and to compensate the decrease of tool diameter.

To support the weight of the tool, springs are used in the bottom of actuator holder, as shown in **section B-B**. Six actuator systems are located cylindrically in the front and rear of actuator holder, as is shown in **section C-C**. The actuator system is composed of a piezoelectric actuator, a load cell, a gap sensor and a supporting pad.

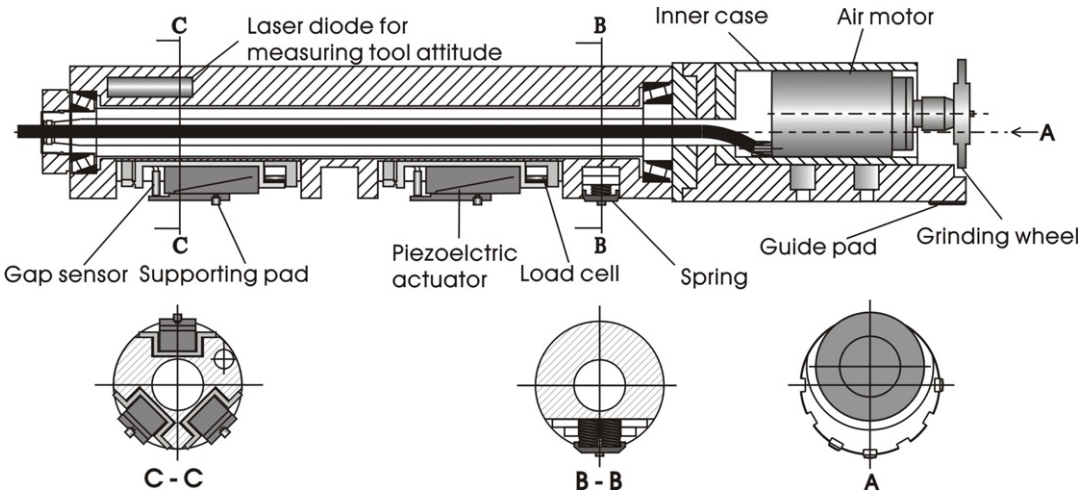

Fig. 2 Laser-guided deep-hole internal grinding tool.

The connection of the inner case to the grinding head is illustrated in **Fig.3**. The inner case connects to the grinding head by four linear guides. By these operations of linear guides, the position of an inner case can be adjusted easily. And two jigs with a spring are fixed to suppress for the displacement of inner case caused by the centrifugal force on grinding.

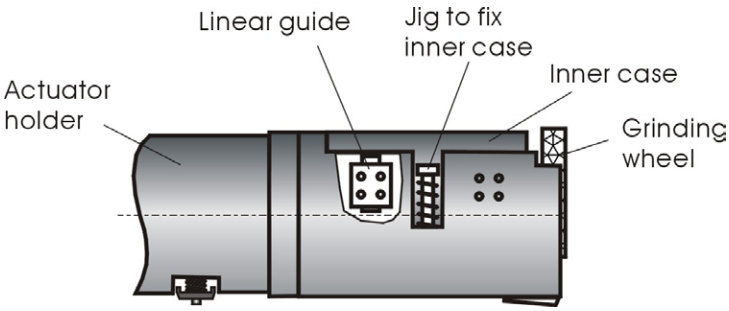

Fig.3 Connection of an inner case to the grinding head.

The principle of grinding is illustrated in **Fig.4**. The grinding is carried out by the rotation of grinding wheel (*Ro*) and the rotation of grinding head (*Re*). Grinding forces can be presented as the normal force (P_N) and the

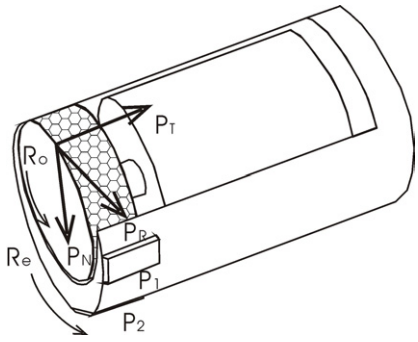

Fig.4 Principle of grinding.

tangential force (P_R).

It is considered that guide pad P_1 supports the tangential force (P_R) and guide pad P_2 supports the normal force (P_N).

The torque T_R on the rotating wheel of radius R by the tangential force P_R is:

$$T_R = R \cdot P_R \qquad (1)$$

3. Grinding Forces

3.1 Experimental procedure and equipment

The experimental system is mainly composed of the NC milling machine and the data acquisition system as shown in **Fig.5**. The system details are as follows:

1. Air motor:
   Output power, 120 W
   Maximum rotational speed, 4800 rpm
   Proper air pressure, 0.3~0.5MPa
   Spindle accuracy, < 2 μ m
   Air consumption, 150Nl/min
   Maximum torque, 1.7N· m
2. Sensing: Dynamometer.
3. Grinding wheel: Diamond wheel (SD80PA5), ϕ82mm×6mm
4. Workpieces material:
   Cemented carbide (JIS B 4053 V 30), High-speed steel (JIS G 4403 SKH 51).

The air motor is placed in the spindle of NC milling machine. To measure grinding forces, a dynamometer is fastened to a machine table. Force signals obtained from the dynamometer are transmitted to the amplifier. The signals are digitalized by an A/D converter and are saved on a personal computer. The rotational speed of grinding wheel is 3000rpm and the feed speed is 1m/min. The depths of cut are 10, 20 and 30μm. The grinding is performed under dry condition.

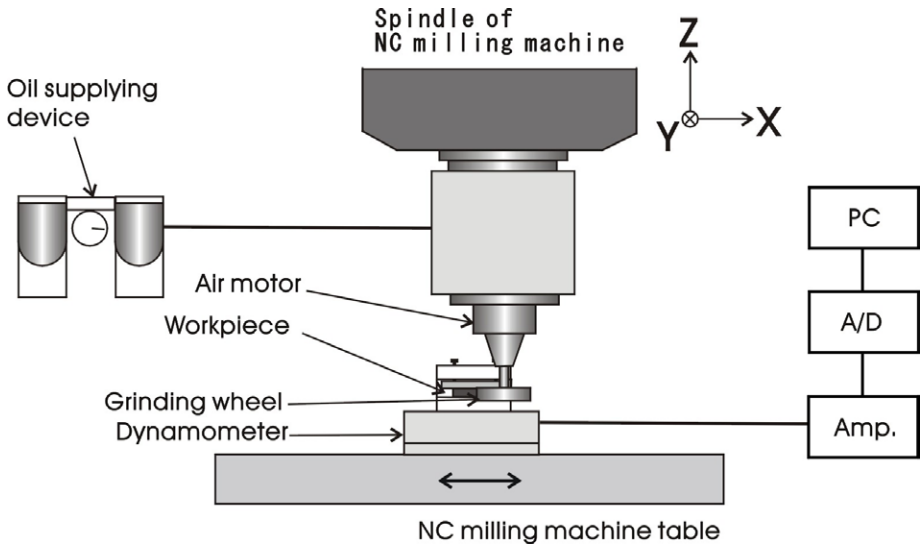

Fig.5 Experimental apparatus.

3.2 Experimental results

The normal and tangential forces per unit width are shown in **Fig.6**.

Figure 6 (a) is the case that cemented carbide is ground. In the case of down grinding, the normal force is initially about 0.1N/mm at a depth of cut of 10 μ m and slightly increases to 1.3N/mm at a depth of cut of 30 μ m. The tangential force is 0.02N/mm at a depth of cut of 10 μ m and increases to 0.5N/mm at a depth of cut of 30 μ m. In the case of up grinding, the normal force is initially about 0.15N/mm at a depth of cut of 10 μ m and slightly increases to 1.2N/mm at a depth of cut of 30 μ m. The tangential force is about 0.05N/mm at a depth of cut of 10 μ m and increases to 0.55N/mm at a depth of cut of 30 μ m.

Figure 6 (b) shows the grinding force when grinding high-speed steel. In the case of down grinding, the normal force was initially about 0.4N/mm at a depth of cut of 10 μ m and slightly increases to 2.8N/mm at a depth of cut of 30 μ m. The tangential force is about 0.1N/mm at a depth of cut of 10 μ m and increases to 1.3N/mm at a depth of cut of 30 μ m. In the case of up grinding, the normal force is initially about 0.5N/mm at a depth of cut of 10 μ m and slightly increases to 3.1N/mm at a depth of cut of 30 μ m. The tangential force is about 0.2N/mm at a depth of cut of 10 μ m and increases to 1.35N/mm at a depth of cut of 30 μ m.

The maximum torque is 0.135N·m when grinding cemented carbide and this comes under 8% of the maximum torque of air motor. When grinding high-speed steel, the maximum torque is 0.3N·m and comes under 20% of the maximum torque of air motor. Generally, a motor can be used if the torque on cutting becomes 80~85% of the maximum torque of the motor. Therefore, the air motor can be used to grind cemented carbide and high-speed steel in the developed grinding head.

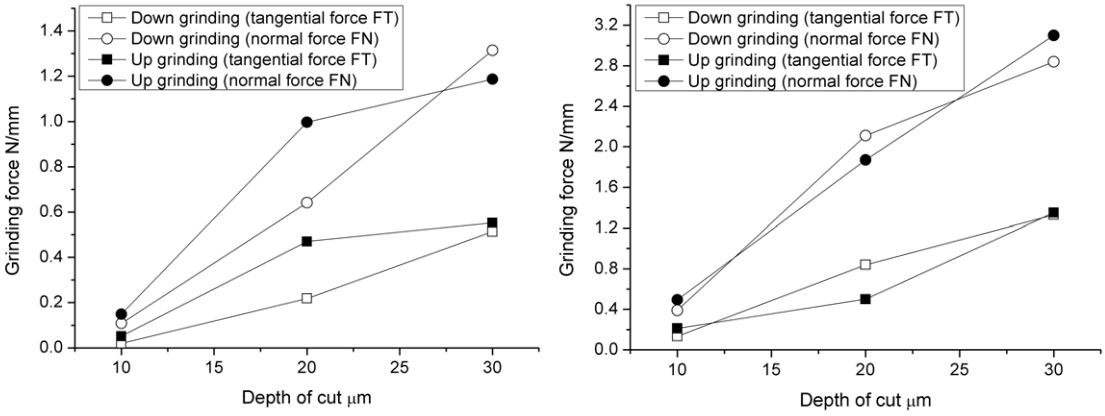

(a) Cemented carbide (b) High-speed steel

Fig.6 Grinding forces.

4. Displacement of a Grinding Wheel and Performance of Piezoelectric Actuators

The model experiments are carried out to examine the displacement of a grinding wheel in detail. Also, the performance of piezoelectric actuators, which are placed under an inner case for compensation of the displacement of a grinding wheel, is examined during grinding.

4.1 Experimental apparatus and method

4.1.1 Displacement of a grinding motor

The experimental apparatus to examine the displacement of a grinding motor and performance

of piezoelectric actuators is shown in **Fig.7**. The workpiece is placed on spindle of NC milling machine. The grinding forces are measured by strain gages stuck on a boring bar, which is fastened to the table of a NC milling machine. The displacement of a grinding motor is measured by an electric micrometer. The forces and the displacement are digitalized by A/D converter and are saved in a personal computer. The tachometer is used to measure variation of the rotational speed of grinding wheel.

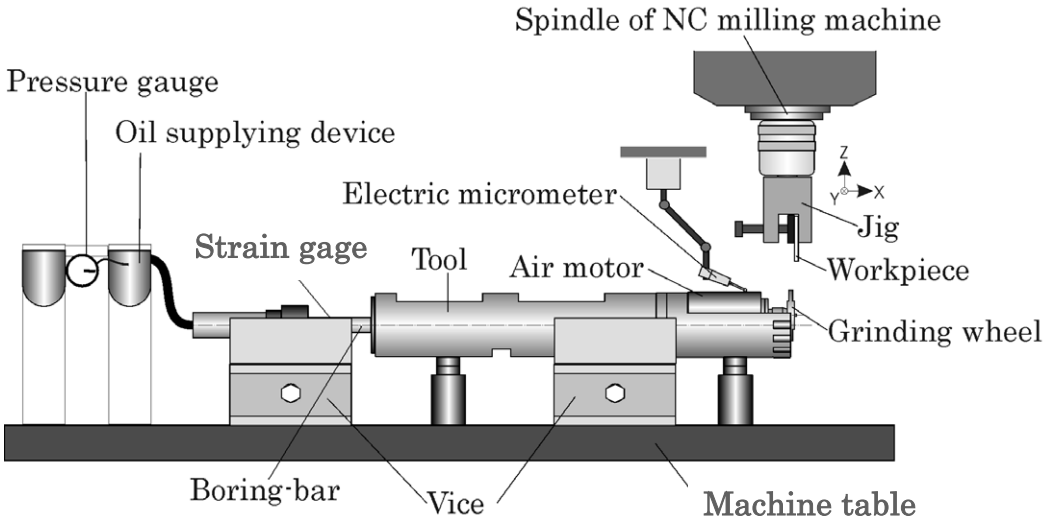

Fig.7 Experimental apparatus.

Table 1 Grinding conditions.

Depth of cut μm	Grinding	Feed speed m/min	Rotational speed rpm
10	Down	1	2200
20			
30			
10	Up		
20			
30			

The grinding conditions are shown in **Table 1**. The cemented carbide is ground under dry condition. The feed speed is 1m/min and the rotational speed of grinding wheel is 2200rpm.

4.1.2 Performance of piezoelectric actuators

The experimental apparatus to examine the performance of piezoelectric actuators is shown in **Fig.8**. To examine the performance of piezoelectric actuators, the relationship between the displacements of a grinding motor, which is caused by the grinding forces and is compensated by piezoelectric actuators, is measured using electric micrometer during grinding. These signals are digitalized by A/D converter and are saved in a personal computer. The voltage impressed from piezoelectric actuator driver.

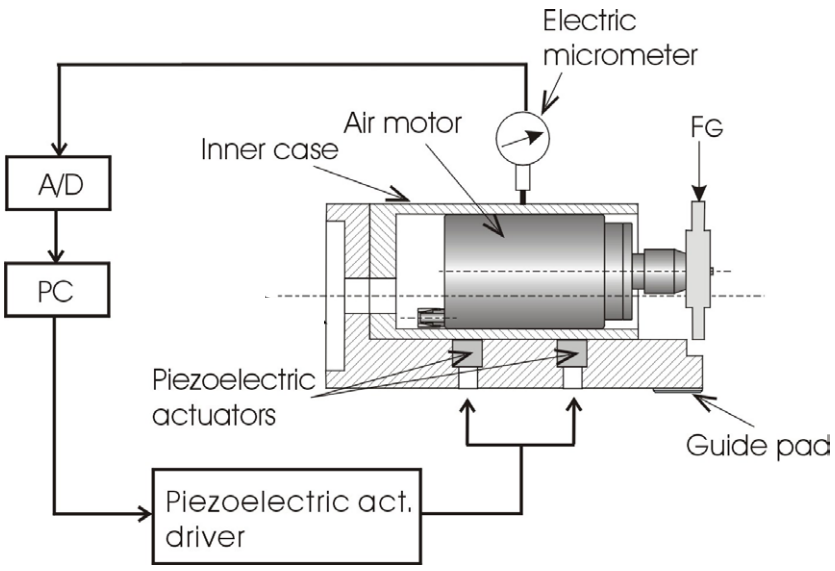

Fig.8 Experimental apparatus for examining the performance of piezoelectric actuators.

Table 2 Grinding conditions.

Depth of cut μm	Feed speed m/min	Rotational speed rpm
200	0.1	2200

The grinding conditions are shown in **Table 2**. A depth of cut is 200 μ m, the feed speed is 0.1m/min and the rotational speed of grinding wheel is 2200rpm. The cemented carbide is ground under dry condition.

4.2 Experimental results

4.2.1 Grinding forces and displacement of the grinding motor

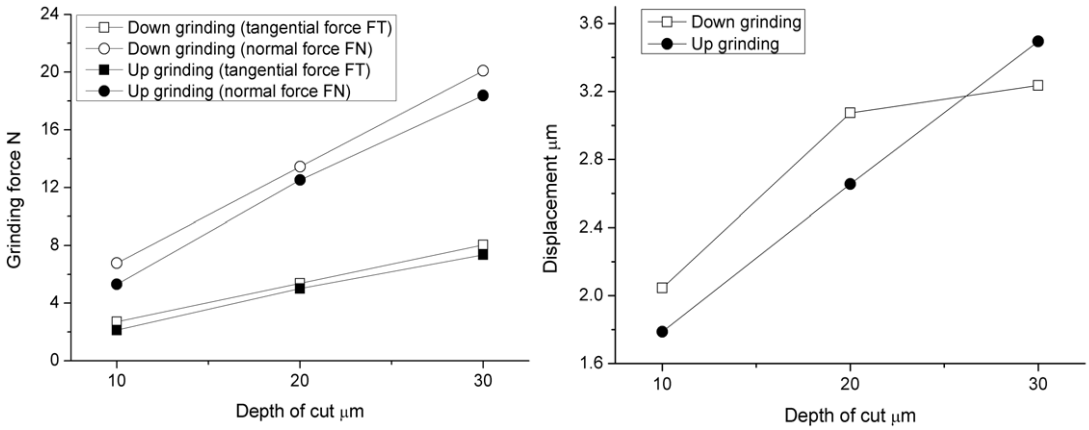

(a) Grinding forces (b) Displacement

Fig.9 Grinding forces and displacement of the grinding motor.

The grinding forces and displacement of a grinding motor during grinding are shown in **Fig.9**. In **Fig.9 (a)**, the normal forces are the values estimated from **Fig.6**. The grinding forces proportionally increase to a depth of cut of 30μm. In the case of down grinding, the tangential force increases from 2.7N to 8N. The normal force increases from 6.7N to 20.1N. In this time, the displacement of the grinding motor is varied from 2.0μm to 3.2μm. In the case of up grinding, the tangential force increases from 2.1N to 7.3N. The normal force increases from 5.3N to 18.4N. The displacement of the grinding motor varies from 1.8μm to 3.5μm.

4.2.2 Performance of piezoelectric actuators

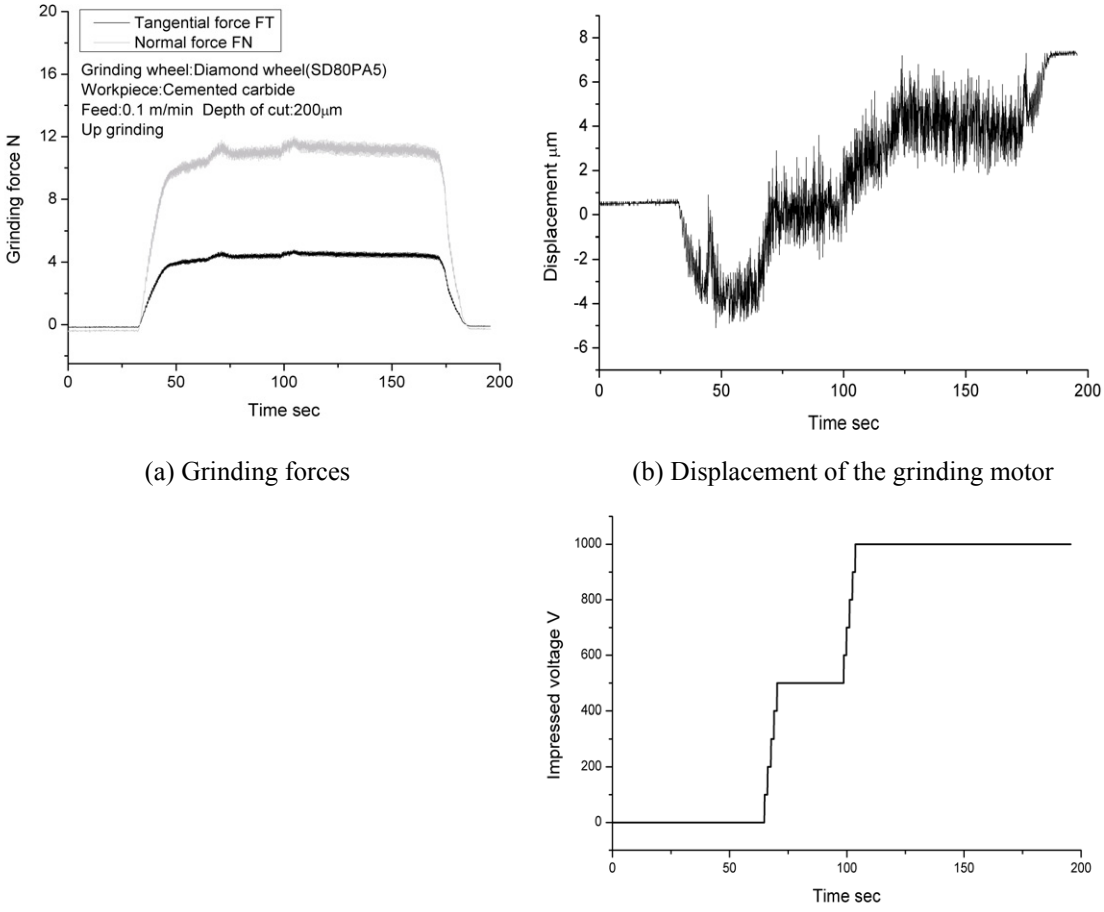

(a) Grinding forces

(b) Displacement of the grinding motor

(c) Impressed voltage

Fig.10 Performance of piezoelectric actuators.

The performance of piezoelectric actuators is shown in **Fig.10**. In **Fig.10 (a)**, the normal force is the value estimated from **Fig.6**. The tangential force is 4N and the normal force is 10N. The displacement of the grinding motor is shown in **Fig.10 (b)**. When the grinding starts, the grinding motor is varied by -4μm. To compensate the displacement, voltage is impressed to each piezoelectric actuator, as is shown in **Fig.10 (c)**. The grinding motor is displaced by +4μm when 500V is impressed to each piezoelectric actuator. When 1000V is impressed to each piezoelectric actuator, the displacement of the grinding motor is varied by +8μm.

5. Stiffness of Air Motor Spindle

5.1 Experimental apparatus

The experimental apparatus to examine the stiffness of air motor spindle is shown in **Fig.11**. A dead weight is exerted a shaft, which is inserted to the chuck with collet of air motor. The diameter of shaft is 6mm. The displacement of air motor spindle is measured on the chuck with collet of air motor using electric micrometer.

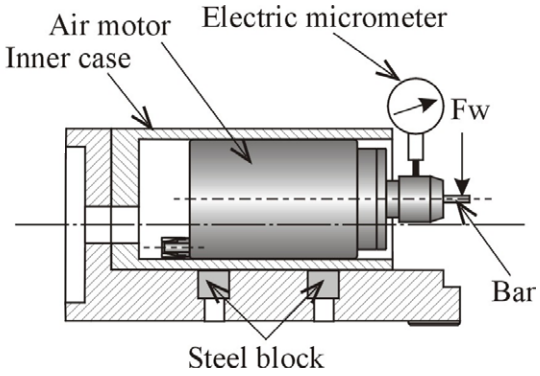

Fig.11 Experimental apparatus.

5.2 Experimental results

The relationship between the displacement of a grinding motor and dead weight acting on it is shown in **Fig.12**. The dead weights are 9, 18, 27 and 36N. The stiffness of air motor spindle is 0.6μm/N.

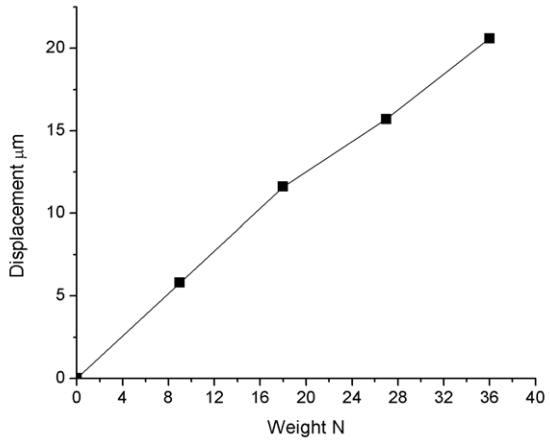

Fig.12 Stiffness of air motor spindle.

6. Internal Grinding on the Lathe

6.1 Experimental apparatus and method

The internal grinding is carried out using grinding head on the lathe. The experimental apparatus is shown in **Fig. 13**. To conduct the experiments under the equivalent grinding condition to the laser-guided internal grinding system, the grinding wheel is rotated by air motor and a

workpiece is rotated by the lathe spindle. The grinding head is connected to the jig with strain gage, which is placed on the table.

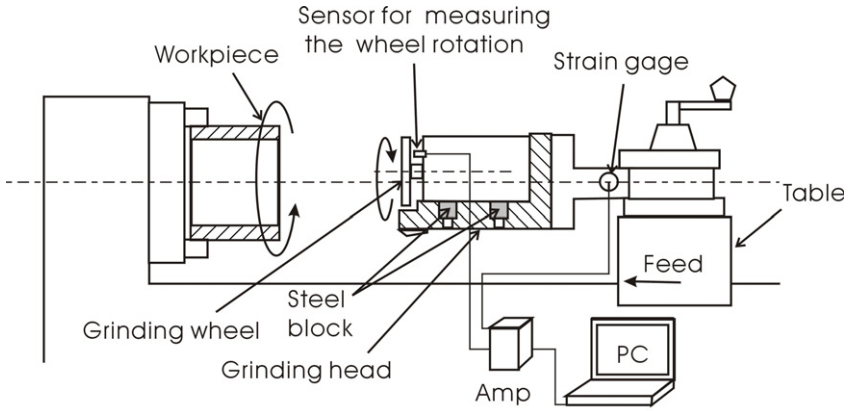

Fig.13 Experimental apparatus.

The grinding wheel is CBN wheel (CBC80V75C) with a diameter of 82mm, a width of 6mm and a grain size of 200 μ m, as is shown in **Fig.14**. To reduce an impact in the time that the grinding is started, a chamfer is made in the grinding wheel.

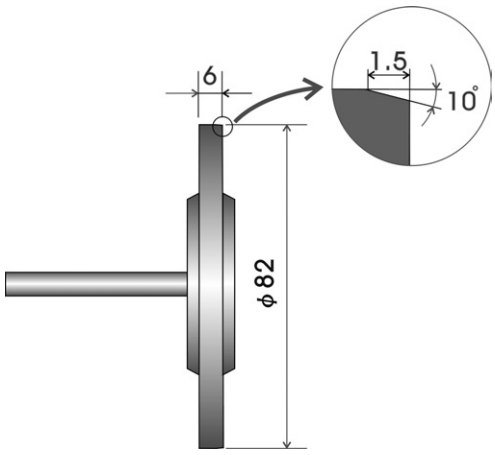

Fig.14 Grinding wheel.

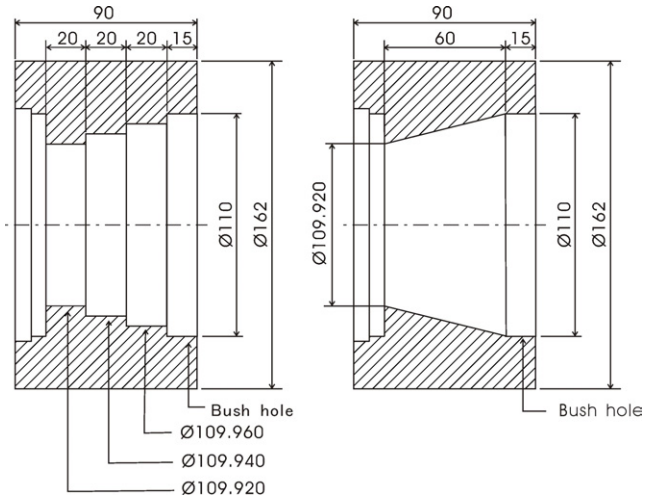

(a) Step shaped (b) Taper shaped

Fig.15 Workpieces (tool diameter: ϕ 109.980mm).

Two kinds of workpieces are shown in **Fig.15**. There are a step shaped workpiece and a taper shaped workpiece. All workpieces have a hole of 110mm dia. for bushing to a depth of 15mm. In the case of the step shaped workpiece, its diameter of prebored hole changes in a step shape from 109.960mm through 109.940mm to 109.920mm. In the case of the taper shaped workpiece, the diameter of prebored hole decreases in a taper shape from 110mm to 109.920mm. And all workpieces are hardened steel (Jis-type S45C) with HRC 55-60.

6.2 Experimental results

The torque and hole deviation in the case that a step shaped workpiece is ground are shown in **Fig.16**. The holes are finished until depth of 65mm. With an increase in a depth of cut, the grinding

torques increase until 0.6, 1.2 and 1.8Nm, which correspond approximately to 27, 54 and 82N of normal forces, respectively. The hole diameters after grinding are109.990mm at a depth of cut of 10μm and 109.980mm at a depth cut of 20μm.

The torque and hole deviation in the case that a taper shaped workpiece is ground are shown in **Fig.17**. The holes are finished until depth of 75mm. With an increase in a depth of cut, the grinding torques increase to 1.4Nm. It is estimated that the tool diameter is 109.990mm because the hole diameter is 109.990mm at a depth of cut 10μm. The hole diameter after grinding is larger than tool diameter until a depth of 25mm and is smaller than tool diameter from depth of 25mm. The hole diameter at depth of 75mm is smaller by 30μm than tool diameter.

The displacement of air motor spindle increases with an increase in a depth of cut. The weak stiffness of air motor spindle is one of cause why hole diameter is smaller than tool diameter. In **Fig.17 (a)**, the grinding torque is 1.3Nm when a depth of cut is 35μm. In this case, the tangential force is 23N and the normal force is 57N. Supposing that the 1/3 torque of total torque is consumed by burnishing between guide pads and hole wall [6], the normal force of grinding wheel is 36N. In this case, the displacement of air motor spindle is 21μm (**Fig.12**).

However, the developed grinding head can be used when a depth of cut is small. When the piezoelectric actuators are used for compensating the displacement of the grinding motor, the diameter of ground hole approaches to that of the grinding head.

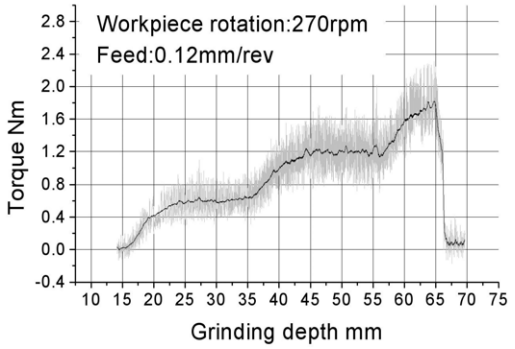

(a) Torque

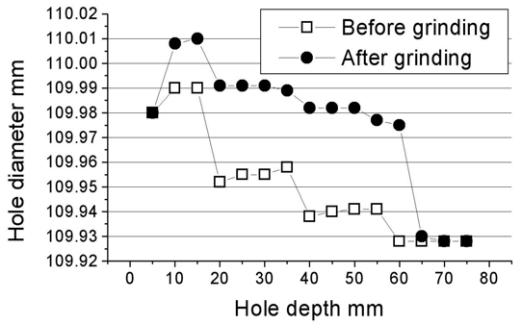

(b) Hole deviation

Fig.16 Step shaped workpiece.

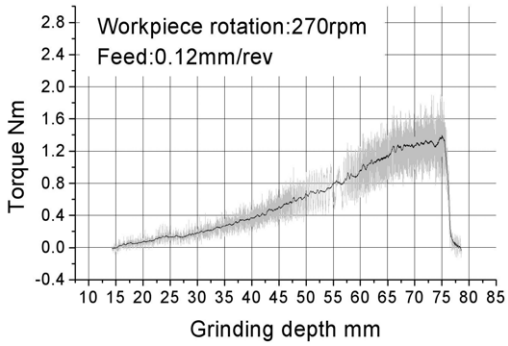

(a) Torque

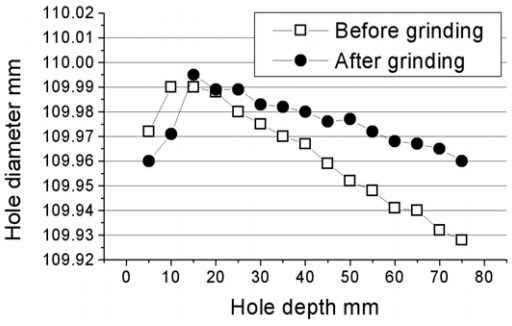

(b) Hole deviation

Fig.17 Taper shaped workpiece.

After each experiment, a heavy loading can be observed on the grinding wheel, as shown in **Figs.18 and 19**. **Figure 19**, i.e. a photo that is taken by SEM, shows chips cut by grains of the grinding wheel. The loading is also one of causes why hole diameter is smaller than tool diameter. It is due to the fact that the compressed air cannot sufficiently remove chips on the grinding wheel.

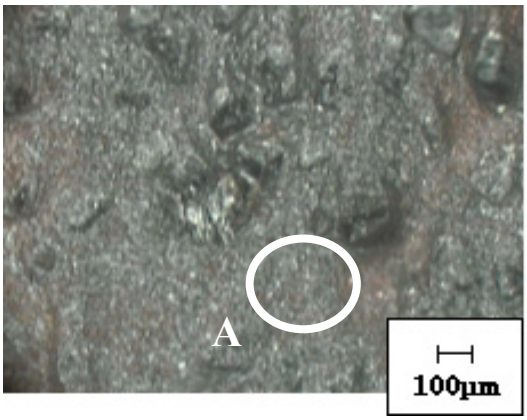

Fig.18 Loading of the CBN wheel.

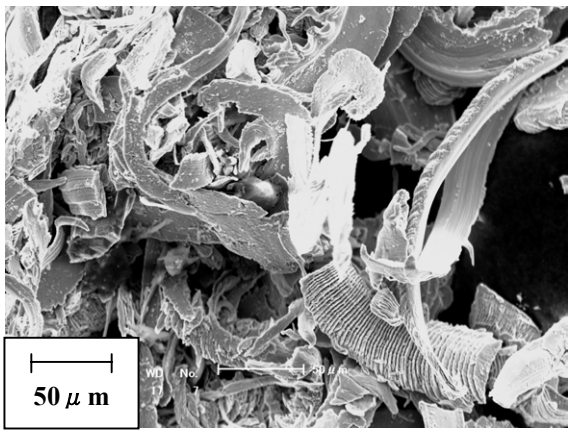

Fig.19 Chips (from area A).

7. Conclusions

The laser-guided deep hole internal grinding tool is designed and fabricated to finish deep hole. With respect to grinding forces, its performance is examined. As a result, it is concluded as follows.

1. The cemented carbide and the high-speed steel are ground sufficiently using air motor. The torque when grinding cemented carbide with a depth of cut of 30μm is 8% of the maximum torque of air motor and the torque when grinding high-speed steel with a depth of cut of 30μm is 20% of the maximum torque of air motor.
2. The displacement of a grinding motor and the normal force are 3.2μm and 20.1N, respectively, when grinding with a depth of cut of 30μm. Its displacement can be compensated by the piezoelectric actuators.
3. The developed grinding head can be used for finishing the deep hole when a depth of cut is small.

In a continued report, performance of the tool is examined on the deep hole drilling machine.

Acknowledgements

We thank Mr. K. Tei and Mr. T. Nakanishi, graduate students and Mr. F. Wakabayashi, an undergraduate student. The observation and picturing of chips were performed by the scanning electron microscope equipped in the Center of Advanced Instrumental Analysis, Kyushu University.

References

1) Jih-hua Chin et al.; The shaft behavior of BTA deep hole drilling tool, Int. J. Mech. Sci., Vol.38, No.5, pp.461-482, 1996.
2) A. Katsuki et al.; 'Development of a high-performance laser-guided deep-hole boring tool: optimal determination of reference origin for precise guiding', Precision Engineering, Vol.24, pp.9-14, 2000.
3) A. Katsuki et al.; 'Development of a Practical High-Performance Laser-Guided Deep-Hole Boring Tool: Improvement of Guiding Strategy', Proc. of euspen International Conference on

Precision Engineering, Micro Technology, Measurement Techniques and Equipment, pp.97-100, 2003.

4) B.K. Min et al.; A smart boring tool for process control, Mechatronics, Vol.12, pp.1097-1114, 2002.
5) W.M. Chiu et al.; Design and testing of piezoelectric actuator-controlled boring bar for active compensation of cutting force induced errors, Int. J. Production Economics, Vol.51, pp.135-148, 1997.
6) R. Richardson, R. Bhatti ; A review of research into the role of guide pads in BTA deep-hole machining, Journal of Materials Processing Technology 110, pp.61-69, 2001.